Available online at www.sciencedirect.com

ScienceDirect

Mendeleev Commun., 2018, **28**, 562–564

Mendeleev Communications

Morphology and composition of NiMoW/P-Al_2O_3 systems based on the modified support with varied P_2O_5 content

Pavel S. Solmanov, Nikolay M. Maximov,* Natalya N. Tomina and Andrey A. Pimerzin

Samara State Technical University, 443100 Samara, Russian Federation. Fax: +7 846 242 3580; e-mail: maximovnm@mail.ru

DOI: 10.1016/j.mencom.2018.09.039

The series of NiMoW/P-Al_2O_3 catalysts with varied P_2O_5 content in their support was synthesized and characterized in their sulfide state by the XPS and HRTEM methods. The absence of phosphorus in the structure of NiMoWS crystallites and its location only on the Al_2O_3 surface were indirectly confirmed. The rate constant values for the hydrodesulfurization and hydrogenation reactions were determined at 275 and 300 °C, while the variation of these values was significant.

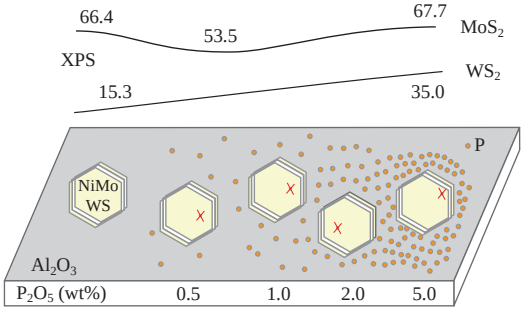

The introduction of inorganic additives in the composition of hydrotreating catalysts is one of the methods to increase their activity. The modification of their support is used, *e.g.*, to change the acid-base properties of catalytic system. The increased or decreased acidity (Brønsted or Lewis) affects the interaction of active phase precursors with the carrier surface,[1–3] the uniformity of their distribution,[4] and the morphology of sulfide phase.[1,5–9] The increased acidity of carrier also raises the efficiency of hydrodenitrogenation (HDN),[10,11] hydrogenation,[5,10,12] and hydrodesulfurization.[3,12] Phosphorus is among the most studied and often applied modifiers.[6–9] The dopation with P_2O_5 provides the increased dispersion of MoS_2, which enhances the catalytic activity of the above catalysts in the HDN and hydrogenation reactions.[8,9]

The series of NiMoW/P-Al_2O_3 catalysts with the different contents of P_2O_5 (0, 0.5, 1.0, 2.0, and 5.0 wt%; molar ratio of Mo:W = 1:1) in the support was prepared and activated.† The obtained catalysts were characterized by the HRTEM and XPS‡ methods that are common for the investigation of solid catalysts.[13–15]

† The modifier was introduced at the first stage of two-step synthesis by the wetness impregnation from an aqueous solution of phosphoric acid. Once the impregnation was finished, the modified carrier was dried at 60, 80, and 110 °C and then calcinated at 550 °C (for 2 h at each temperature). The $H_3PMo_{12}O_{40}\cdot nH_2O$ and $H_3PW_{12}O_{40}\cdot nH_2O$ heteropolyacids and nickel citrate were used as the precursors of Mo, W and Ni sulfides, respectively [molar ratio of $NiO:(MoO_3+WO_3)$ = 1:2]. The modified support containing P_2O_5 (up to 5 wt% per Al_2O_3, Table 1) was impregnated with aqueous solution of active phase precursors (Mo, W, and Ni) at the second step of synthesis and dried at 60, 80, and 110 °C (for 2 h at each temperature).

The catalyst samples were activated by sulfidation in a H_2/H_2S stream ($H_2:H_2S$ = 30:70 v/v) at 500 °C for 2 h.

‡ The XPS spectra were recorded on a Kratos Axis Ultra DLD spectrometer using a monochromatic Al K source ($h\nu$ = 1486.6 eV, 150 W). The collected spectra were processed using the CasaXPS program (Version 2.3.16) after the performed Shirley background subtraction and Gaussian (30%)–Lorentzian (70%) decomposition parametrization. The appropriate oxide and sulfided references as supported monometallic catalysts were used during the decompositions of the Ni 2*p*, Mo 3*d*, W 4*f* and S 2*p* XPS spectra.

The chemical species occupying the surface of sulfided samples were examined by XPS. The decomposition of Ni 2*p* spectra§ acquired on sulfided NiMoW/P-Al_2O_3 catalysts (Figure 1) revealed the percentile fractions of Ni, Mo and W metal species presented on the surface of sulfided NiMoW/P-Al_2O_3 catalysts (Figure 2).

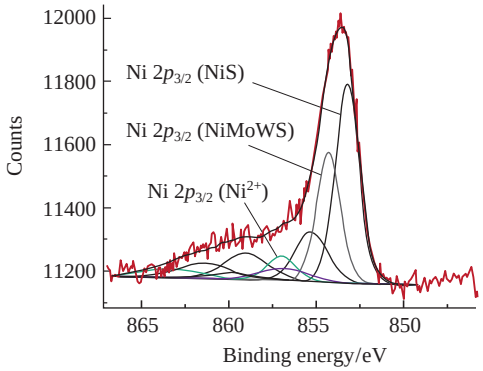

Figure 1 The decomposition of Ni 2*p* spectra recorded for the NiMoW/P-Al_2O_3 catalysts.

Table 1 Morphological characteristics of the NiMoWS phase species, calculated from TEM micrographs.

P_2O_5 (wt%)	Average length/nm	Average stacking number	Dispersion of Ni(Mo)(W)S
0.0	3.8	2.0	0.31
0.5	4.0	2.0	0.29
1.0	3.2	2.1	0.36
2.0	3.1	2.2	0.37
5.0	4.8	2.3	0.25

§ For more details, see Online Supplementary Materials.

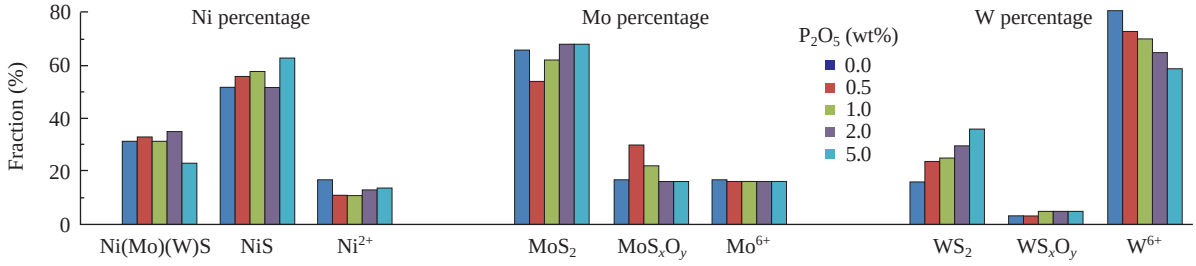

Figure 2 Percentile fractions based on the XPS data for Ni, Mo and W metal species in the sulfided NiMoW/P-Al_2O_3 catalysts.

The increased content of phosphorus in the support slightly affects the ratio of Ni [Ni^{2+}, NiS, and Ni(Mo)(W)S] species, except for the decreased (to 23%) fraction of NiMoWS species and the consequently increased (to 63%) proportion of NiS species in the case of sample with the P_2O_5 content of 5.0 wt%. According to the previously reported data,[16,17] the transformation of tungsten oxide into sulfide cannot be completed under the typical conditions of full sulfurization of Mo catalysts (400 °C). The complete conversion of WO_3 into WS_2 occurs only at higher temperatures (up to 1000 °C),[18] which agrees well with the experimental data acquired in this work. The facilitated capability of W-species of undergoing sulfidation under the conditions of more preferable formation of Ni(Mo)(W)S phase has been already demonstrated in the case of presence of Mo and Ni.[19] Since the W species are sulfided at higher temperature than Ni and Mo ones, the higher concentration of Ni(Mo)(W)S phase corresponds to the samples with higher (Ni + Mo)/W ratios, while in the case of lower (Ni + Mo)/W ratios, the patterns are lower and segregated sulfide phases of Ni and W or WO_xS_y are present. The (Ni + Mo)/W ratio will vary for the catalysts containing the different amount of phosphorus, since a part of nickel fraction can form phosphates at the hydrothermal stage of synthesis, which are very stable and unreducible at higher temperatures.[20] The ratios of Mo (Mo^{6+}, MoS_xO_y, and MoS_2) species deviate significantly for the samples with 0.5 and 1.0 wt% of P_2O_5. The decreased proportion of Mo^{6+} particles was observed along with increasing the proportion of MoS_xO_y particles. The linear increase in the proportion of WS_2 (from 15 to 35%) was observed (see Figure 2) for tungsten species in the case of the higher content of phosphorus, accompanied with the correspondingly decreased W^{6+} fraction (from 81 to 59%).

The determination of atomic ratio of P : Al on the surface was based on the XPS data (Figure 3). The dependence of this ratio on the total phosphorus content in the catalyst is described by the linear function with the approximated confidence value of 0.97. This fact indirectly indicates the absence of phosphorus in the structure of NiMoWS crystallites and its location on the surface of Al_2O_3.

The acquired HRTEM data allowed us to estimate the average dimension of NiMoWS active phase,¶ which was varied from 3.1 to 4.8 nm, and the average stacking number of slabs of NiMoWS grows varied from 2.0 to 2.3 upon increasing P_2O_5 content (up to 5 wt%) (see Table 1). The sample with P_2O_5 content of 5.0 wt% demonstrated the lowest dispersion of active phase species equal to 0.25. The patterns of samples with P_2O_5 content of 1.0 and 2.0 wt% exhibited the highest dispersion (0.36–0.37). Thus, the dispersion of the active phase, which is a derivative of layer length and of number of layers in the sulfide phase, is the most informative characteristic of morphology of the active phase. As shown hereinafter, the samples possessing the highest dispersion demonstrated the highest catalytic activity.

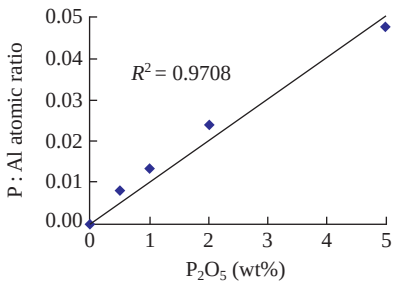

Figure 3 P : Al atomic ratio *vs.* P_2O_5 content for NiMoW/P-Al_2O_3 catalysts.

The catalytic activity of samples was determined for the hydrotreating process [bench-scale flow reactor, T = 275 or 300 °C, liquid hourly space velocity (LHSV) = 60 h^{-1}, P = 3.0 MPa, H_2/feed = 300/1 $nm^3\,m^{-3}$] of model mixtures (MM): (i) dibenzothiophene (DBT) (0.3 wt%) in toluene (MM-1); (ii) DBT (0.3 wt%), naphthalene (1.5 wt%), and quinoline (0.5 wt%) (MM-2). The catalytic activities were estimated *via* the values of DBT hydrodesulfurization (HDS) rate constants (pseudo-first order kinetic models):

$$k_{HDS}^{DBT} = W \ln \frac{C_0}{C},$$

where W is LHSV (h^{-1}), C_0 is the DBT feed concentration, and C is the DBT product concentration (wt%).

The changes in the catalytic activity of samples in the hydrogenolysis of dibenzothiophene and hydrogenation (HYD) of naphthalene reactions were significant, while their maximum was observed in the case of P_2O_5 content of 0.5–1.0 wt% (Figure 4). The rate constant values of these reactions were in the range of 29.4–54.4 h^{-1} at 275 °C and in the range of 67.6–110.0 h^{-1} at 300 °C for various catalysts. The k_{HDS} value varied from 29.9 to 49.8 h^{-1} at 275 °C and from 24.9 to 51.1 h^{-1} at 300 °C for the reaction of DBT hydrogenolysis in the presence of quinoline and naphthalene. The hydrogenation rate constant (k_{HYD}) varies from 1.09 to 2.20 at 275 °C and from 2.20 to 3.21 h^{-1} at 300 °C in the case of naphthalene hydrogenation.

The catalytic activity of samples in the DBT HDS and naphthalene HYD reactions reaches its maximum at the P_2O_5 content

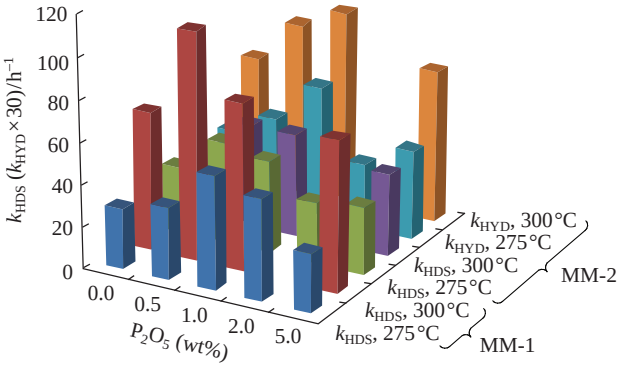

Figure 4 Relationship between DBT k_{HDS} (naphthalene k_{HYD}) and P_2O_5 content for NiMoW/P-Al_2O_3 catalysts.

¶ The original HRTEM images and the approach used for their processing are given in Online Supplementary Materials.

of 0.5–1.0 wt%. Note that in the previous tests of PNiMo-containing samples, the maximal HDS and HYD activities of vacuum gas oil hydrotreating were also observed for this P_2O_5 content (*i.e.*, 0.5–1.0 wt%). This fact can be probably explained by the either absence or presence of high-molecular polycyclic aromatic hydrocarbons and nitrogen-containing species.

The adsorption of organic sulfur compounds is competing with the nitrogen-containing compounds and polyaromatic hydrocarbons. In the case of small number of adsorption sites (*i.e.*, the Lewis sites with π-adsorption mechanism for the residual sulfur-containing compounds), the HDS reactions occur to a small extent, while the reactions involving high-molecular nitrogen-containing compounds and polyaromatic hydrocarbons are suppressed to a lesser extent. This is due to the minimal activity in the case of hydrodesulfurization of vacuum gas oil.

The correspondence between changes in the atomic ratio of P:Al determined by XPS on the surface and those in the phosphorus content also indirectly indicates that the phosphorus is not included in the structure of NiMoWS crystallites and located on the Al_2O_3 surface. Probably, those phosphorus species could change the conditions of competitive adsorption of sulfur-containing compounds, nitrogen-containing compounds, and polyaromatic hydrocarbons and affect the HDS, HYD and HDN activities of catalysts. The changed amount of phosphorus in the catalyst results in the changed amount and strength of acid sites on its surface, hence the strength of adsorption of the reacting compounds varies. In the presence of a small number of strongly acidic centres, the competition for them between the sulfur, aromatic and nitrogen compounds leads to the strong adsorption of basic nitrogen compounds and their derivatives, which can be of interest as affecting the hydrogen recombination rate at low temperatures. In the presence of a large number of acidic centres of medium or low strength, the displacement of basic nitrogen compounds by the weakly binding sulfur and aromatic ones becomes possible, which may be caused by both the concentration and thermal factors under the reaction conditions. Nevertheless, the acidity of samples is changing upon the variations of phosphorus amount and affecting both the adsorption of reactants and performance of spillover effect in the reaction medium.

The presence of naphthalene and quinoline does not practically suppress DBT HDS at 275 °C, while the DBT conversions in the case of using MM-2 at 275 °C and 300 °C are close to each other. This could be probably explained by the higher temperature (300 °C, less than 1 wt%) needed for the HDN reactions, while quinoline was only converted to tetrahydroquinoline without any HDN at 275 °C. It is also possible that the tetrahydroquinoline adsorption on the hydrogenation sites leads to the more difficult recombination of activated hydrogen and consequently, the direct desulfurization reaction can be expended. Subsequent increases in the temperature promote the activated hydrogen recombination, which is expressed in the decreased HDS rate constant. This temperature effect for hydrogen spillover was also reported earlier.[21] The possibility of σ-sites formation during the HDS[22] is doubtful since the DBT adsorption would be sterically hindered.[23] One the one hand, the increased temperature leads to the HDS acceleration, while on the other hand, the lower concentration of activated hydrogen compensates this effect.

This work was supported by the Russian Foundation for Basic Research (grant no. 16-33-60094 mol_a_dk). The authors are grateful to P. A. Nikul'shin for his assistance in the processing of XPS spectra.

Online Supplementary Materials

Supplementary data associated with this article can be found in the online version at doi: 10.1016/j.mencom.2018.09.039.

References

1 U. Usman, M. Takaki, T. Kubota and Y. Okamoto, *Appl. Catal. A*, 2005, **286**, 148.
2 G. Li, W. Li, M. Zhang and K. Tao, *Appl. Catal. A*, 2004, **273**, 233.
3 Y. Saih and K. Segawa, *Catal. Today*, 2003, **86**, 61.
4 S. Damyanova, L. Dimitrov, L. Petrov and P. Grange, *Appl. Surf. Sci.*, 2003, **214**, 68.
5 D. Ferdous, A. K. Dalai, J. Adjaye and L. Kotlyar, *Appl. Catal. A*, 2005, **294**, 80.
6 D. Ferdous, A. K. Dalai and J. Adjaye, *J. Mol. Catal. A*, 2005, **234**, 169.
7 R. Huirache-Acuña, B. Pawelec, E. Rivera-Muñoz, R. Nava, J. Espino and J. L. G. Fierro, *Appl. Catal. B*, 2009, **92**, 168.
8 C. Liu, Y. Yu and H. Zhao, *Fuel Process. Technol.*, 2004, **86**, 449.
9 Usman, T. Yamamoto, T. Kubota and Y. Okamoto, *Appl. Catal. A*, 2007, **328**, 219.
10 L. Ding, Z. Zhang, Y. Zheng, Z. Ring and J. Chen, *Appl. Catal. A.*, 2006, **301**, 241.
11 N. Kunisada, K.-H. Choi, Y. Korai, I. Mochida and K. Nakano, *Appl. Catal. A*, 2005, **279**, 235.
12 C.-E. Hédoire, E. Cadot, F. Villain, A. Davidson, C. Louis and M. Breysse, *Appl. Catal. A*, 2006, **306**, 165.
13 I. S. Mashkovsky, P. V. Markov, G. O. Bragina, G. N. Baeva, A. V. Rassolov, A. V. Bukhtiyarov, I. P. Prosvirin, V. I. Bukhtiyarov and A. Yu. Stakheev, *Mendeleev Commun.*, 2018, **28**, 152.
14 P. V. Markov, G. O. Bragina, A. V. Rassolov, I. S. Mashkovsky, G. N. Baeva, O. P. Tkachenko, I. A. Yakushev, M. N. Vargaftik and A. Yu. Stakheev, *Mendeleev Commun.*, 2016, **26**, 494.
15 W. Trakarnpruk, *Mendeleev Commun.*, 2016, **26**, 256.
16 E. J. M. Hensen, Y. van der Meer, J. A. R. van Veen and J. W. Niemantsverdriet, *Appl. Catal. A*, 2007, **322**, 16.
17 Y. van der Meer, E. J. M. Hensen, J. A. R. van Veen and A. M van der Kraan, *J. Catal.*, 2004, **228**, 433.
18 Y. Okamoto, A. Kato, Usman, N. Rinaldi, T. Fujikawa, H. Koshika, I. Hiromitsu and T. Kubota, *J. Catal.*, 2009, **265**, 216.
19 S. L. González-Cortés, S. Rugmini, T. Xiao, M. L. N. Green, S. M. Rodulfo-Baechler and F. E. Imbert, *Appl. Catal. A*, 2014, **475**, 270.
20 S. Soled, S. Miseo, J. Baumgartner, J. Guzman, T. Bolin and R. Meyer, *Catal. Today*, 2015, **246**, 3.
21 M. Villarroel, P. Baeza, F. Gracia, N. Escalona, P. Avila and F. J. Gil-Llambías, *Appl. Catal. A*, 2009, **364**, 75.
22 V. A. Salnikov, P. A. Nikulshin and A. A. Pimerzin, *Petrol. Chem.*, 2013, **53**, 233 (*Neftekhimiya*, 2013, **53**, 267).
23 M. Egorova and R. Prins, *J. Catal.*, 2006, **241**, 162.

Received: 13th February 2018; Com. 18/5477